Borehole breakout and drilling-induced fracture analysis from image logs

M. Tingay, J. Reinecker, and B. Müller

Introduction

Borehole breakouts and drilling-induced fractures (DIFs) are important indicators of horizontal stress orientation, particularly in aseismic regions and at intermediate depths (<5 km). Approximately 19 % of the stress orientation indicators in the World Stress Map (WSM) database have been determined from borehole breakouts and DIFs. Furthermore, borehole breakouts and DIFs provide the majority of stress orientation indicators in petroleum and geothermal systems. Herein we present a broad overview of the procedures for interpreting borehole breakouts and DIFs from image log data and for WSM quality ranking of stress orientations derived from these features.

Borehole Breakouts

Borehole breakouts are stress-induced enlargements of the wellbore cross-section (Bell and Gough, 1979). When a wellbore is drilled, the material removed from the subsurface is no longer supporting the surrounding rock. As a result, the stresses become concentrated in the surrounding rock (i.e. the wellbore wall). Borehole breakout occurs when the stresses around the borehole exceed that required to cause compressive failure of the borehole wall (Zoback et al., 1985; Bell, 1990). The enlargement of the wellbore is caused by the development of intersecting conjugate shear planes that cause pieces of the borehole wall to spall off (Figure 1). The stress concentration around a vertical borehole is greatest in the direction of the minimum horizontal stress (S_h). Hence, the long axes of borehole breakouts are oriented approximately perpendicular to the maximum horizontal compressive stress orientation (S_H; Plumb and Hickman, 1985).

Drilling-Induced Fractures

DIFs are created when the stresses concentrated around a borehole exceed that required to cause tensile failure of the wellbore wall (Aadnoy, 1990). DIFs typically develop as narrow sharply defined features that are sub-parallel or slightly inclined to the borehole axis in vertical wells and are generally not associated with significant borehole enlargement in the fracture direction (note that DIFs and breakouts can form at the same depth in orthogonal directions). The stress concentration around a vertical borehole is at a minimum in the S_H direction. Hence, DIFs develop approximately parallel to the S_H orientation (Figure 1; Aadnoy and Bell, 1998).

Introduction to Borehole Imaging Tools

Borehole imaging tools provide an image of the borehole wall that is typically based on physical property contrasts. There are currently a wide variety of imaging tools available, though these predominately fall into two categories: resistivity and acoustic imaging tools.

Resistivity imaging tools provide an image of the wellbore wall based on resistivity contrasts (Ekstrom et al., 1987). Resistivity imaging tools have evolved from dipmeter tools and consist of four- or six-caliper arms with each arm ending with one or two pads containing a number of resistivity buttons. Resistivity image tools provide the same information on borehole diameter and geometry as the older

dipmeter tools, however the resistivity buttons also allow high-resolution resistivity images of the borehole wall to be developed (see WSM four-arm caliper log guidelines for a detailed description of dipmeter tools and associated log data). There are a wide variety of wireline resistivity imaging tools available, some of the more common tools are the Formation Micro Scanner (FMS; from Schlumberger), Formation Micro Imager (FMI; from Schlumberger), Oil-Based Micro Imager (OBMI; from Schlumberger), Simultaneous Acoustic and Resistivity tool (STAR; from Baker Atlas), Electrical Micro Scanner (EMS; from Halliburton) and Electrical Micro Imager (EMI; from Halliburton). Furthermore, recent years have seen the development of a range of logging while drilling (LWD) or measurement while drilling (MWD) resistivity image logging tools, such as the Resistivity At Bit (RAB; from Schlumberger) and STARtrak (from Baker Inteq). For more details on resistivity image logging tools see Ekstrom et al (1987) or Asquith and Krygowski (2004).

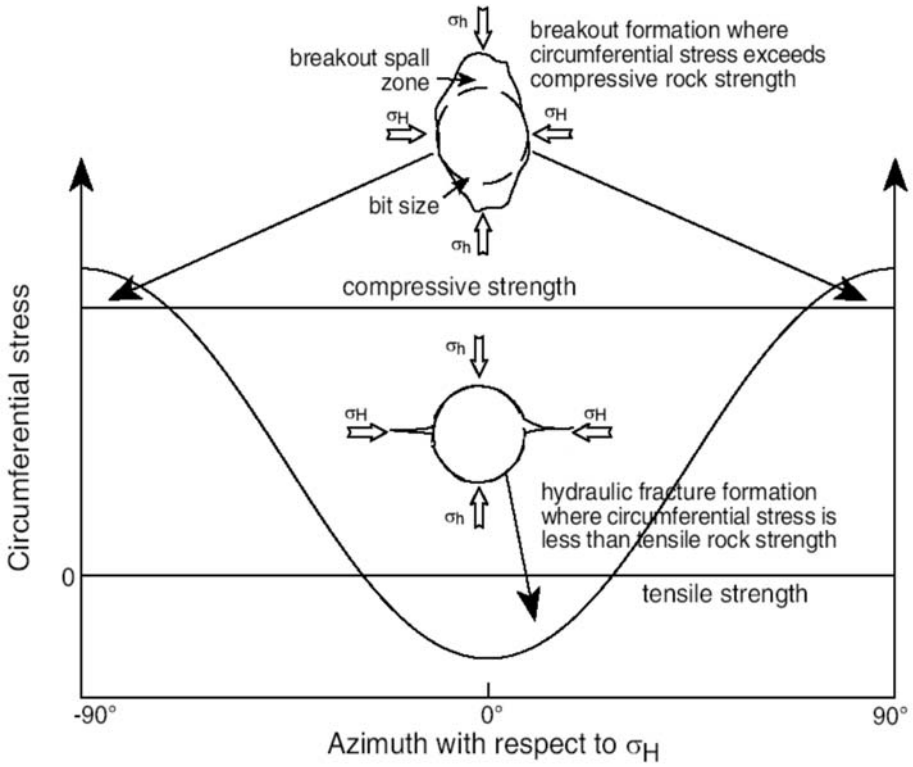

Figure 1: Schematic cross-sections of borehole breakout and drilling-induced fracture (DIF; figure adapted from Hillis and Reynolds, 2000). Borehole breakouts form when the circumferential stress around the wellbore exceeds the compressive rock strength and thus are oriented parallel to the minimum horizontal stress (σ_h). DIFs form when the circumferential stress exceeds the tensile strength of the wellbore wall and are thus oriented parallel to the maximum horizontal stress (σ_H).

Acoustic imaging tools utilise a rapidly rotating piezoelectric transducer to emit a focused high-frequency sonic pulse to the borehole wall (Asquith and Krygowski, 2004). The acoustic imaging tool then records the amplitude of the return echo as well as the total travel time of the sonic pulse. The acoustic wave travel time and reflected amplitude is measured at numerous azimuths inside the wellbore for any given depth. This data is then processed into images of the borehole wall reflectance (based on return echo amplitude) and borehole radius (based on pulse travel time). There are a wide variety of acoustic imaging tools available, some of the more common tools are the Borehole Televiwer (BHTV, from Schlumberger), Ultrasonic Borehole Imager (UBI; from Schlumberger), Circumferential Borehole Imaging Log (CBIL; from Baker Atlas), Simultaneous Acoustic and Resistivity tool (STAR; from Baker Atlas), Circumferential Acoustic Scanning Tool-Visualization

(CAST-V; from Halliburton) and the LWD/MWD AcoustiCaliper tool (ACAL; from Halliburton). For more details on acoustic image logging tools see Asquith and Krygowski (2004).

In addition to resistivity and acoustic image logging tools, there are a range of other, currently less common, tools that also provide images of the borehole wall and which may be used for borehole breakout and DIF analysis. Optical image logging tools, such as the Optical Televiewer (from Schlumberger) and Downhole Video tool (from Downhole Video), are wireline tools that utilise cameras to directly image the wellbore wall. Finally, borehole breakouts and DIFs can also be interpreted from MWD/LWD density imaging tools, which provide information on bulk density and photoelectric factor (Pe) at a variety of azimuths around the wellbore and can be used to develop formation density and Pe images. LWD/MWD density image logging tools include the Azimuthal Density Neutron Vision (adnVision; from Schlumberger), Lithotrak (from Baker Inteq) and Azimuthal Lithodensity tool (ALD; from Halliburton).

Interpreting Breakouts and DIFs from Resistivity Image Data

Resistivity image logging tools provide the same information of borehole diameter and geometry as the older dipmeter logs and, thus, this data can be used to interpret breakouts in the same way as for four- or six-arm caliper logs (see WSM guidelines on four-arm caliper analysis). However, resistivity imaging logs also provide a high-resolution picture of the wellbore wall based on resistivity contrasts that allows for the direct observation of borehole breakout. Borehole breakout typically appears on resistivity image logs as broad, parallel, poorly resolved conductive zones separated by 180º (i.e. observed on opposite sides of the borehole) and often exhibiting caliper enlargement in the direction of the conductive zones (Figure 2; Bell, 1996). Breakouts are typically conductive and poorly resolved because the wellbore fracturing and spalling associated with the breakout results in poor contact between the tool pads and the wellbore wall, which in turn causes the tool to partially or fully measure the resistivity of the electrically conductive drilling mud rather than the formation . However, it is important to note that breakouts will appear as resistive, rather than conductive, zones in resistivity images run in oil-based mud (such as using the OBMI tool).

Drilling-induced fractures can only be observed on image logs. DIFs typically become infiltrated by drilling mud and, thus, appear on resistivity image logs as pairs of narrow, well defined conductive features (resistive in oil-based mud images) separated by 180º (Figure 3; Aadnoy and Bell, 1998). Furthermore, unlike natural fractures that tend to cross-cut the wellbore, DIFs are usually aligned sub-parallel or slightly inclined to the borehole axis in vertical wells (Figure 3).

Interpreting Breakouts and DIFs from Acoustic Image Data

Borehole breakouts are typically interpreted from acoustic image log data using the borehole radius (or travel time) image in combination with images of the reflected amplitude. Borehole breakouts appear as broad zones of increased borehole radius (or travel time) observed on opposite sides of the borehole (Figure 4a). However, breakouts typically have rough and variable surfaces and thus can also often be observed on reflected amplitude images as broad zones of low amplitude (Figure 4a).

Drilling-induced fractures are primarily observed on the reflected amplitude image. Both natural and drilling-induced fractures are poor reflectors of acoustic energy. Hence, DIFs appear as narrow zones of low reflectivity separated by 180º and typically sub-parallel or slightly inclined to the borehole axis (Figure 4b). DIFs are not commonly associated with any borehole enlargement and thus are often not well exhibited on borehole radius images. However, both natural and drilling-induced fractures may appear on borehole radius images as narrow zones of increased borehole radius (Figure 4b).

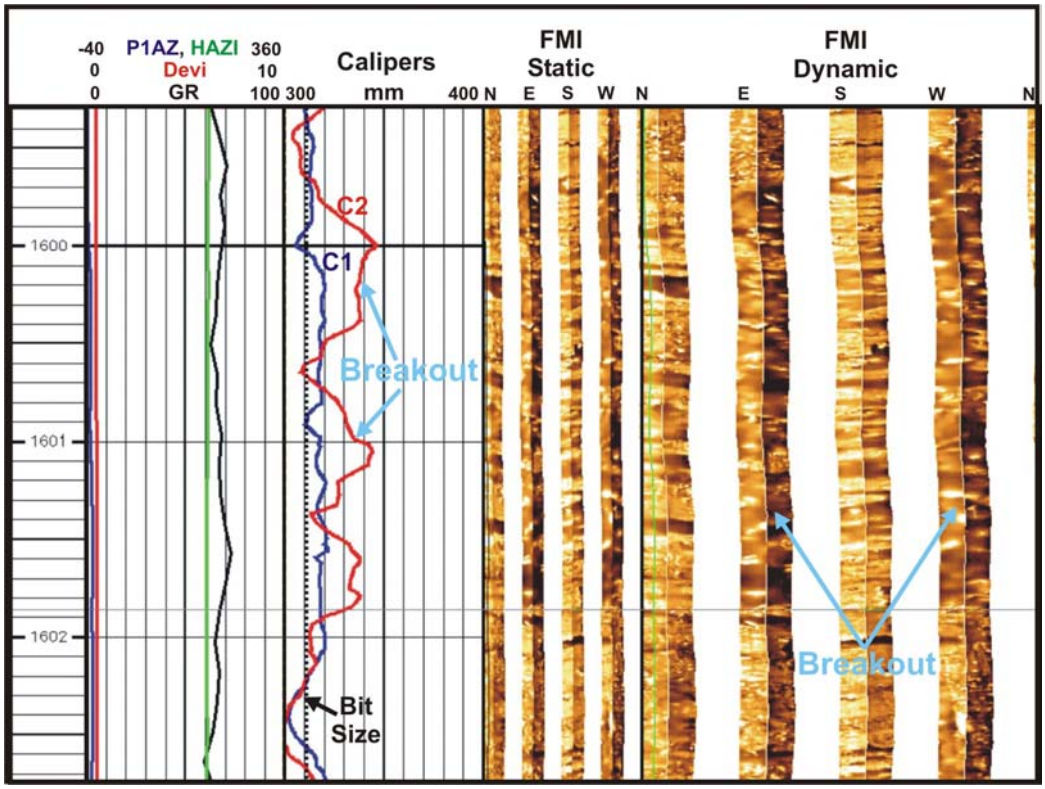

Figure 2: Example of borehole breakout interpreted on a Formation Micro Imager (FMI) log. Breakout is observed both via enlargement in the caliper 2 direction (C2 in red) and directly on the FMI image as broad poorly resolved conductive zones oriented towards 100ºN and 290ºN. These breakouts indicate an approximately N-S maximum horizontal stress orientation.

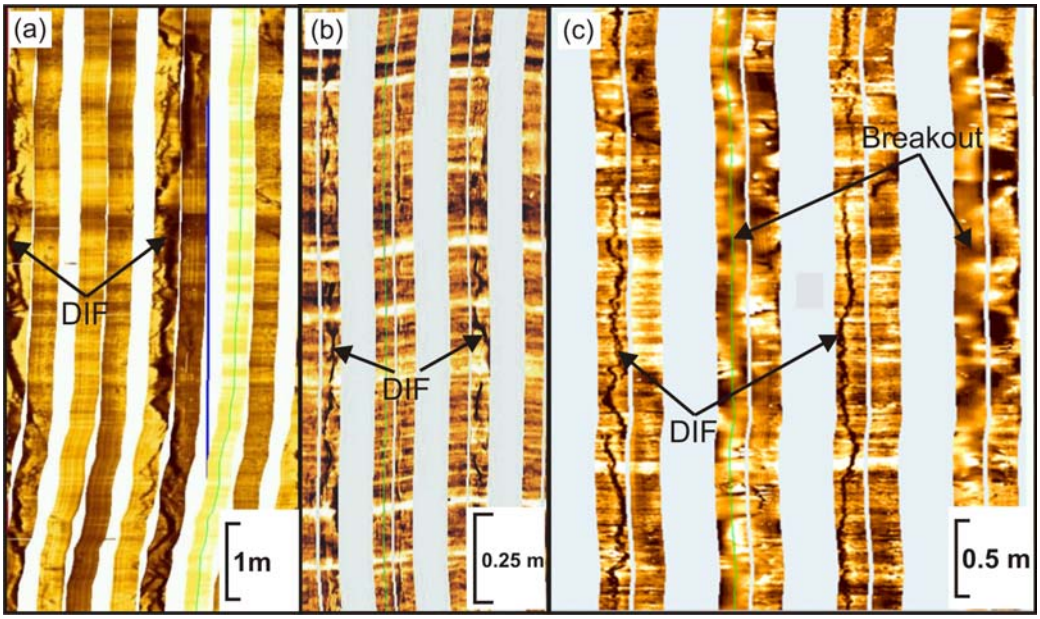

Figure 3: Example of drilling-induced fractures (DIFs) interpreted on Formation Micro Imager (FMI) logs. DIFs are observed as narrow well defined conductive features separated by 180° and oriented sub-parallel to the borehole axis. (a) DIFs are oriented towards 010ºN and 190ºN, indicating an approximately N-S maximum horizontal stress orientation. (b) DIFs are oriented towards 040ºN and 220ºN, indicating an approximately NE-SW maximum horizontal stress orientation. (c) DIFs are oriented towards 045ºN and 225ºN. Furthermore, breakouts are also observed co-incident with the DIFs. Both the breakouts and DIFs indicate an approximately NE-SW maximum horizontal stress orientation.

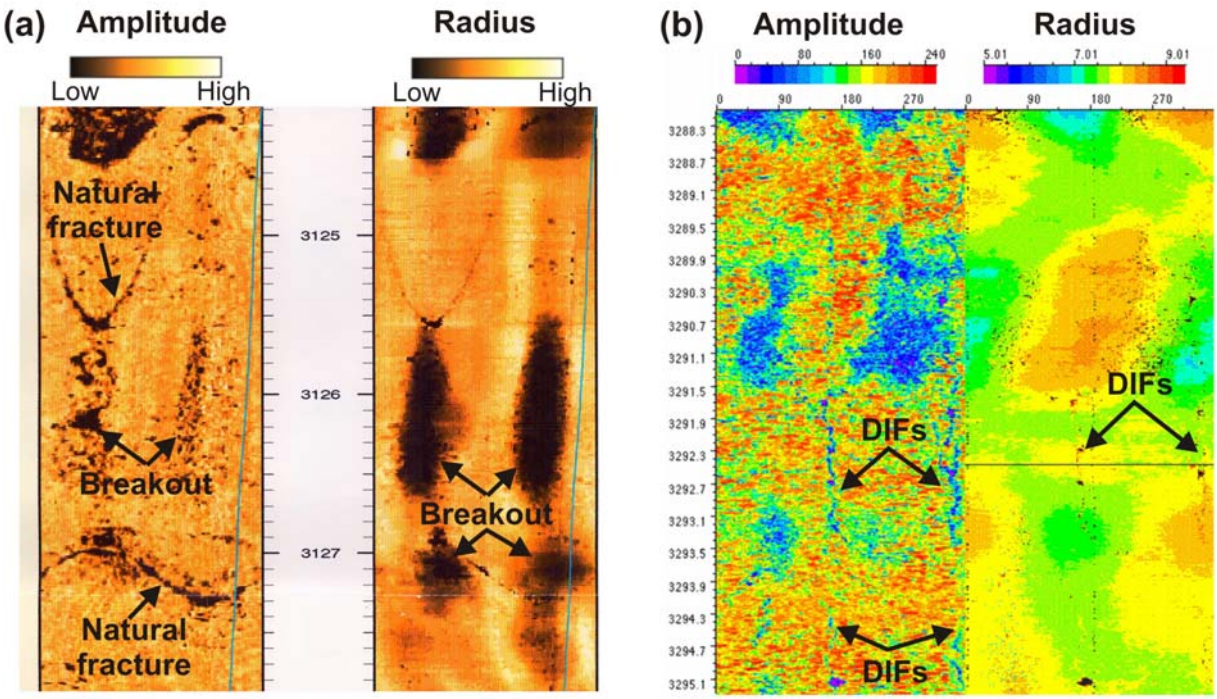

Figure 4: Example of breakouts and drilling-induced fractures (DIFs) observed on acoustic image logs. (a) Borehole breakouts observed on Ultrasonic Borehole Imager log. Borehole breakouts are broad zones of high borehole radius and, to a lesser extent, low reflection amplitude oriented towards 095-275ºN. The borehole breakouts indicate that the present-day maximum horizontal stress is oriented approximately N-S. (b) Borehole Televiewer log showing DIFs oriented towards 165-345ºN. DIFs are observed as zones of low amplitude (left image) and, to a lesser extent, higher radius (right image). The DIFs indicate that the present-day maximum horizontal stress is oriented approximately SSE-NNW.

Interpreting Breakouts and DIFs from Other Image Data

Borehole breakouts and DIFs can also be interpreted from optical image logs and density image logs. On optical image logs (e.g. optical televiewer and Downhole Video), breakouts appear as broad zones of borehole enlargement on opposing sides of the well, while DIFs appear as narrow fractures usually separated by 180º (Figure 5). Density imaging logs, like resistivity imaging logs, require the tool to have direct contact with the wellbore wall. Hence, the density imaging tool partially or fully samples the drilling mud rather than the wellbore wall in breakout and DIF zones. Drilling mud is less dense than the formation and hence breakouts appear as broad low density zones separated by 180 degrees (Figure 6), while DIFs are sometimes visible as narrow low density axial-parallel fractures on bulk density images. However, many drilling muds also contain barite, which has an extremely high photoelectric absorption factor. Hence, breakouts can also be observed as broad zones of high photoelectric absorption on Pe images (Figure 6), while DIFs appear as narrow high Pe fracture zones oriented sub-axial to the wellbore.

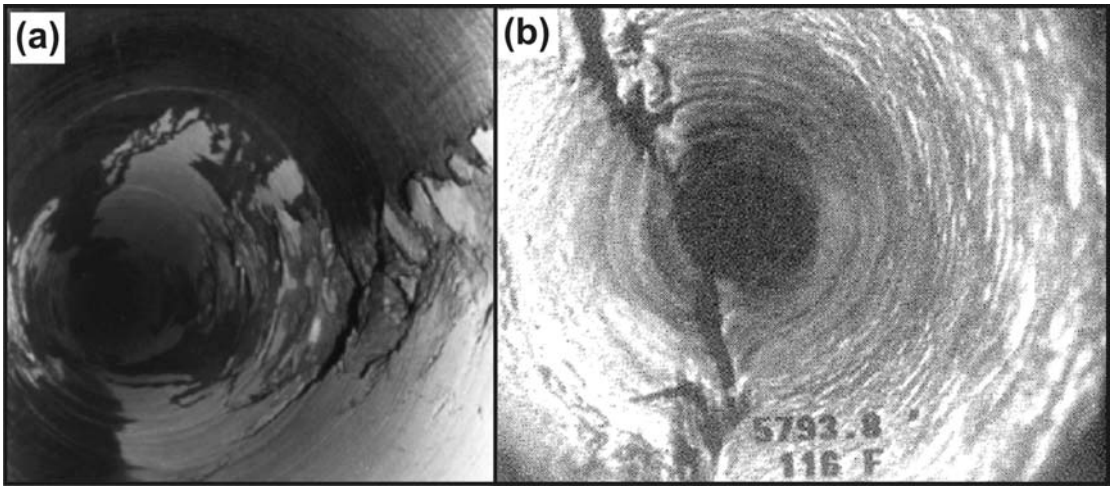

Figure 5: (a) Example of borehole breakout taken by a downhole camera. (b) Example of a borehole fracture observed on a downhole camera (Figure 4(b) from Asquith and Krygowski, 2004).

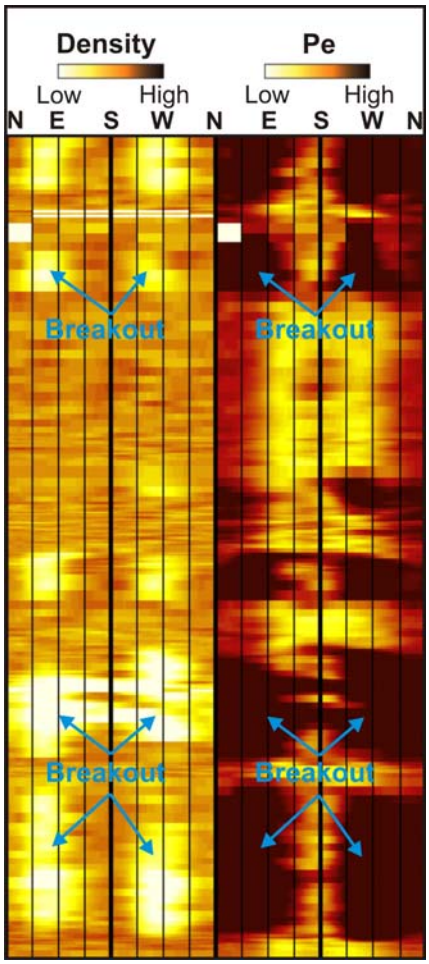

Figure 6: Example of breakouts on density and photoelectric absorption factor (Pe) images from a LWD/MWD Azimuthal Lithodensity tool. Breakouts show up as pairs of broad poorly resolved zones separated by 180° that have low density and high Pe. The breakouts are oriented approximately 060-240°N and indicate that the present-day maximum horizontal stress is oriented approximately ENE-WSW.

Determining the Average Maximum Horizontal Stress Orientation: Circular Statistics

BO and DIF orientations are bimodal data. Data between 180° and 360° are equivalent to those from the interval 0-180° (S_H varies between 0 and 180°). According to Mardia (1972) the mean breakout azimuth θ_m (i.e. S_h) of a population of n picked breakout long axis directions θ_i is derived by first transforming the angles to the 0-360° interval.

$$\theta_i^* = 2\ \theta_i$$

Then the direction cosine and sine of θ_i^* has to be added and averaged either by the number of measurements (for number weighted mean) or weighted by the BO or DIF length and then divided by the total BO or DIF length L (length weighted mean).

number weighted:

$$C = \frac{1}{n}\sum_{i=1}^{n} \cos\theta_i^*$$

$$S = \frac{1}{n}\sum_{i=1}^{n} \sin\theta_i^*$$

length weighted:

$$L = \sum_{i=1}^{n} l_i$$

$$C = \frac{1}{L}\sum_{i=1}^{n} l_i \cos\theta_i^*$$

$$S = \frac{1}{L}\sum_{i=1}^{n} l_i \sin\theta_i^*$$

where l_i is the length of BO or DIF i with orientation θ_i^*.

The mean azimuth results from: $\theta_m = ½ \arctan(S/C)$

(Make sure that the angles are converted from rad into deg!)

The standard deviation s_o is derived as

$$s_o = 360/2\pi\ (-1/2\ \log_e R)^{1/2} \quad \text{with} \quad R = (C^2 + S^2)^{1/2}.$$

World Stress Map Quality Ranking

All data in the WSM database are quality ranked to facilitate comparison between different indicators of stress orientation (e.g. focal mechanism solutions, overcoring). Image logs provide a much more reliable interpretation of borehole breakouts than four-arm caliper logs. Therefore, stress orientations determined from BO and DIFs interpreted on image log data are quality ranked separately. The quality-ranking criteria are presented in Table 1 and Table 2. Note that BO and DIFs must be treated separately during quality ranking. For example, a well that exhibits both BO and DIFs will receive two stress indicators, one for the stress orientation determined from the BO and another for the stress orientation determined from DIFs.

Table 1: WSM quality ranking criteria for breakouts interpreted from image logs in a single well (s.d. = standard deviation).

A-Quality	B-Quality	C-Quality	D-Quality	E-Quality
≥ 10 distinct breakout zones and combined length ≥ 100 m in a single well with s.d. ≤ 12°	≥ 6 distinct breakout zones and combined length ≥ 40 m in a single well with s.d. ≤ 20°	≥ 4 distinct breakout zones and combined length ≥ 20 m in a single well with s.d. ≤ 25°	< 4 distinct breakout zones or < 20 m combined length with s.d. ≤ 40°	Wells without reliable breakouts or with s.d. > 40°

Table 2: World Stress Map quality ranking criteria for drilling-induced fractures interpreted from image logs in a single well (s.d. = standard deviation).

A-Quality	B-Quality	C-Quality	D-Quality	E-Quality
≥ 10 distinct DIF zones and combined length ≥ 100 m in a single well with s.d. ≤ 12°	≥ 6 distinct DIF zones and combined length ≥ 40 m in a single well with s.d. ≤ 20°	≥ 4 distinct DIF zones and combined length ≥ 20 m in a single well with s.d. ≤ 25°	< 4 distinct DIF zones or < 20 m combined length with s.d. ≤ 40°	Wells without reliable DIFs or with s.d. > 40°

References

Aadnoy, B.S. (1990): Inversion technique to determine the in-situ stress field from fracturing data. - J. Petrol. Sci. Engin., **4**, 127-141.

Aadnoy, B.S. and J.S. Bell (1998): Classification of drill-induce fractures and their relationship to in-situ stress directions. - Log Analyst, **39**, 27-42.

Asquith, G. and D. Krygowski (2004): Basic well log analysis. - AAPG Methods in Exploration 16, AAPG, Tulsa, Oklahoma, 244 p.

Bell, J.S. and D.I. Gough (1979): Northeast-southwest compressive stress in Alberta: Evidence from oil wells. - Earth Planet. Sci. Lett., **45**, 475-482.

Bell, J.S. (1990): The stress regime of the Scotian Shelf offshore eastern Canada to 6 kilometres depth and implications for rock mechanics and hydrocarbon migration. - *In:* Maury, V. and D. Fourmaintraux, eds., Rock at Great Depth, Rotterdam, Balkema, 1243-1265.

Bell, J.S. (1996): Petro Geoscience 1. In situ stresses in sedimentary rocks (part 1): measurement techniques. - Geoscience Canada, **23**, 85-100.

Ekstrom, M.P., C.A. Dahan, M.Y. Chen, P.M. Lloyd and D.J. Rossi (1987): Formation imaging with microelectrical scanning arrays. - Log Analyst, **28**, 294-306.

Hillis, R.R and S.D. Reynolds (2000): The Australian Stress Map. - J. Geol. Soc., London, **157**, 915-921.

Mardia, K.V. (1972): Statistics of directional data: probability and mathematical statistics. - 357 pp., London (Academic Press).

Plumb, R.A. and S.H. Hickman (1985): Stress-induced borehole elongation: A comparison between the Four-Arm Dipmeter and the Borehole Televiewer in the Auburn Geothermal Well. - J. Geophys. Res., **90**, 5513-5521.

Zoback, M.D., D. Moos, L.G. Mastin and R.N. Anderson (1985): Well bore breakouts and in situ stress. - J. Geophys. Res., **90**, 5523-5530.